Scientific Research Publishing

Engineering, 2023, 15, 749-758
https://www.scirp.org/journal/eng
ISSN Online: 1947-394X
ISSN Print: 1947-3931

Residual Stress and Fracture Toughness Study in A516 Gr70 Steel Joints Welded and Repaired by Arc Processes

Régis de Matos Curvelo de Barros, Mauricio David Martins das Neves

Center for Materials Science and Technology-IPEN, Energetyc and Nuclear Research Institute (IPEN), São Paulo University, São Paulo, Brazil
Email: barros017@hotmail.com, mdmneves@gmail.com

How to cite this paper: de Barros, R.de M.C. and das Neves, M.D.M. (2023) Residual Stress and Fracture Toughness Study in A516 Gr70 Steel Joints Welded and Repaired by Arc Processes. *Engineering*, **15**, 749-758.
https://doi.org/10.4236/eng.2023.1511052

Received: October 15, 2023
Accepted: November 25, 2023
Published: November 28, 2023

Abstract

Structural components made of steel are used in several areas and require welding for assembly. In some situations, repair of the weld bead, also performed by electric arc welding, can be used to correct, and eliminate any discontinuities. However, electric arc welding causes the presence of residual stresses in the joint, which can impair its performance and not meet specific design requirements. In this paper, welded joints made of ASTM A 516 GR 70 steel plates, with a thickness of 30.5 mm, welded by the MAG—Metal Active Gas process (20% CO_2) and using a "K" groove were analysed. The joints were manufactured with seven welding passes on each side of the groove. After welding, one batch underwent repair of the bead by TIG welding (Tungsten Insert Gas) and another batch underwent two repairs by TIG welding. Were presented results of the behaviour of the residual stress profile measured by X-ray diffraction and the Vickers microhardness profile in the joints as well the fracture toughness in the conditions only welded and submitted to repairs. The results indicated that the greater number of repair passes reduced the residual compressive stress values obtained in the material manufacturing process and caused a stabilization on the Vickers hardness values. It was concluded that compressive residual stresses did not play a major role in the R-curve results. The presence of discontinuities in the welded joint caused greater influence on the behaviour of the R curve.

Keywords

Weld Repair, Weld Fatigue, Weld J Integral, Residual Stress, Microharness

1. Introduction

Structures such as pressure vessels, oil platforms and aircraft fuselage must be

able to maintain their integrity in the most adverse operating conditions, resisting both static and dynamic efforts [1]. In this context the joining process by welding is of great relevance since it serves as a joining process for various parts applied in the afore mentioned branches of knowledge [2]. Repair is understood as the act of promoting a new thermal input that will cause only the fusion of the bead surface, but with less thermal input than welding [3]. The welding process can induce residual stresses, welding defects and changes in the geometric specifications of the joint. In many cases, weld repair can be used to correct such discontinuities [4].

Residual stress is defined as the stress existing in a body without being requested by external agents or significant temperature gradients, considering that the material system is in equilibrium since the sum of forces and moments in the analysed region is zero [4] [5].

Thus, repair can increase the fatigue life of the welded joint eliminating discontinuities creating a surface with greater agreement on the bead, reducing the presence of brittle microstructure and reducing residual stresses [5].

The fracture toughness indicates the ability of the material to absorb energy before catastrophically failing in the presence of a crack or crack-like defect [6]. Additionally change in residual stress due to the joining process is related to the hardness of the material and its fracture toughness.

Another factor that alters material properties is the manufacturing process of the unwelded material. In general, mechanical forming processes such as rolling, bending and extrusion have as their main mechanism for generating residual stresses the heterogeneity of plastic deformations between the various regions of the components. The surface regions are most likely to have compressive residual stresses while the central region presents tensile residual stress and modification of local hardness. Thus, compressive stresses are generated on the surface and tensile stresses in the central region of the part as a reaction of the external fibers to the effort of the central fibers to return to the initial position [7].

Completely, A516 GR70 steel, which has considerable ductility (30% elongation and hardening exponent of 0.2372), thus presenting a high capacity for absorbing strain energy. However, welding and repair of joints using electric arc processes can cause the appearance of residual stresses as well as changing ductile tear test results (R curves) [8] [9] [10]. The aim of this work is to analyse the behaviour of residual stress, microhardness, and J-R curves in welded and repaired joints [11].

2. Materials and Methods

ASTM A516 Gr70 cold rolled steel sheets, 30.5 mm thick and 100 mm long, were welded using the MAG process, using a mixture of argon with 20% active gas (CO_2) as a shielding gas and a flow rate of 13 l/min according to the **Table 1** data.

Three sets of plates were prepared with a K-bevel (to allow full penetration due to the thickness), as shown in **Figure 1(a)**.

Table 1. Welding data detail.

Value	Parameter
Electroder diameter	2.4 mm
Welding current	170 A
DDP	19.0 volts
Wire feeding speedy	15 cm/min
Welding speed	2.5 cm/min
Protection gas	20% CO_2 80% argon – 13.0 l/min
Polarity	DCRP
Deposition	Short-circuit

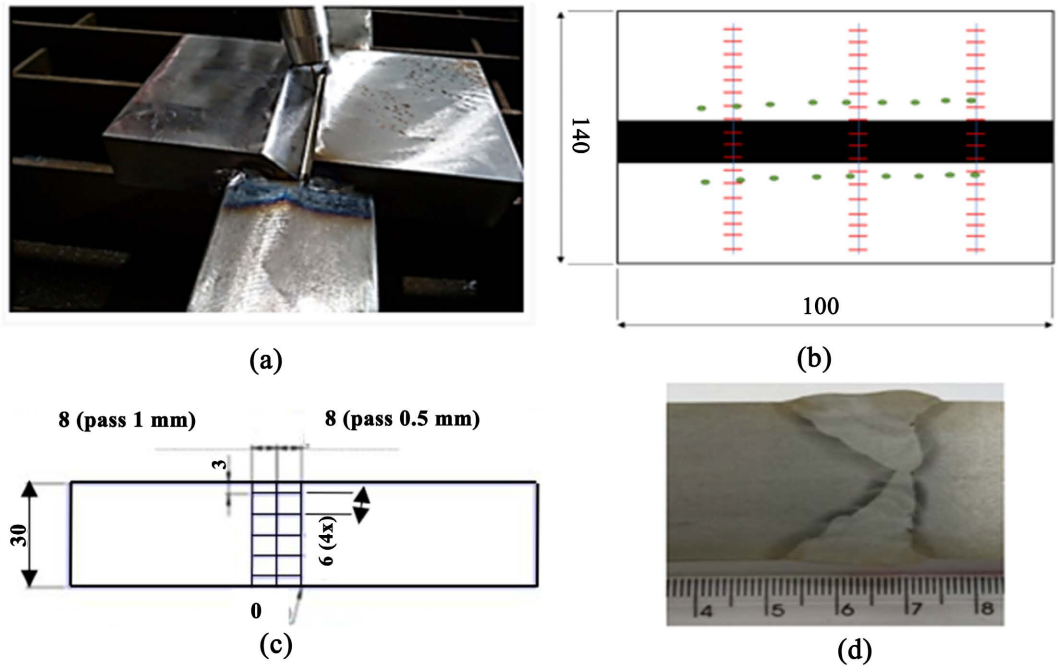

Figure 1. (a) K-groove and MAG weld process and the weld of root. (b) Schematic representation longitudinal and transversal residual stresses measuring points. (c) Schematic representation of microhardness measurements. The dimensions indicate the longitudinal step adopted for the 16 points measurement using a digimess 400 - 310 machine, being 1 mm in the base material (8 points) and 0.5 mm in the HAZ (8 points) totalling 16 measurement points per row, with transverse distance between each measurement row was 6 mm. (d) Image of the cross section of the welding joint after attack with nital etching (2%).

All blanks received seven weld passes on each side of the joint and a ceramic back was implemented to avoid liquid metal leak at the root. MAG welding parameters were current intensity 170 A, direct current with Direct Current Reverse Polarity (DCRP), voltage of 19 V, welding speed 2.5 cm/min, wire feed speed 15 cm/min, Merit wire with diameter of 2.4 mm. After welding the three blanks, only the surface of the weld bead was repaired in two assemblies using the TIG process. The welding conditions used in the repair process were current of 130 A with Direct Current Straight Polarity (DCSP), voltage 7.1 V, inert gas

(argon) flow of 10 l/min, tungsten electrode (2.0% ThO_2) with a diameter of 2.5 mm and torch advance speed of 1.5 cm/s. The repair was done by hand and the temperature after each pass was measured and reached 300˚C in the HAZ region.

After the repair step the three assemblies were named by without repair, one repair pass and two repair passes.

To measure the residual stress series of three rows with 18 points in the longitudinal direction (140 mm dimension direction) of the welding bead and two rows of 9 points in the transversal (100 mm dimension direction) direction of the welding bead all equidistant were marked on the surface of the plate, as shown in Figure 1(b).

In the center of the weld bead, a line of symmetry was considered for the three joint conditions. From the line of symmetry measurements of residual stress on the surface of the sample were performed. To measure the residual stresses was used a RIGAKU model SmartLab X-ray diffraction equipment with a NEX QC+ data acquisition system.

The Vickers hardness measurements were carried out in the cross section of the joint close to the surface of the material, 16 equidistant points, from the reference line of the center of the bead as show in Figure 1(c). The durometer used was from Digmess and the load used was 1 kgf according to ABNT 6507. An example of the result of weld process is exemplified in the joint macrograph in Figure 1(d).

The samples were prepared using metallography techniques to observe the microstructure using optical microscopy. The attack used on the samples was Nital (2% HNO_3).

For the R-curve test, SE(B) specimens were prepared from the respective welded blanks according to ASTM E1820. Slices with a thickness of 15 mm were obtained, totaling three specimens per condition making 9 specimens in total as illustrated by Figure 2(a). The R-curve tests included SE(B) specimens with a notch made by wire electro erosion (tip radius 1.6 mm) whose geometry followed the ASTM E1820 (2021) standard. The pre-crack was performed with a tension of 10% of the yield strength with a frequency of 100 Hz The test was conducted on the MTS universal testing machine with tree points bending (showed by Figure 2(b)) and so that the bending force was applied and caused the crack induced by the initial notch to propagate across the cross section. The electroerosion groove and final dimensions of specimens is showed in detail in Figure 2(a).

3. Results

When analysing the residual stress data in a width direction of 140 mm, starting with the base material, passing through the HAZ, weld metal and ending with the base material (Figure 3) it is noted that it tends not to present such different values between the repair conditions. On the other hand, as a higher level of repair

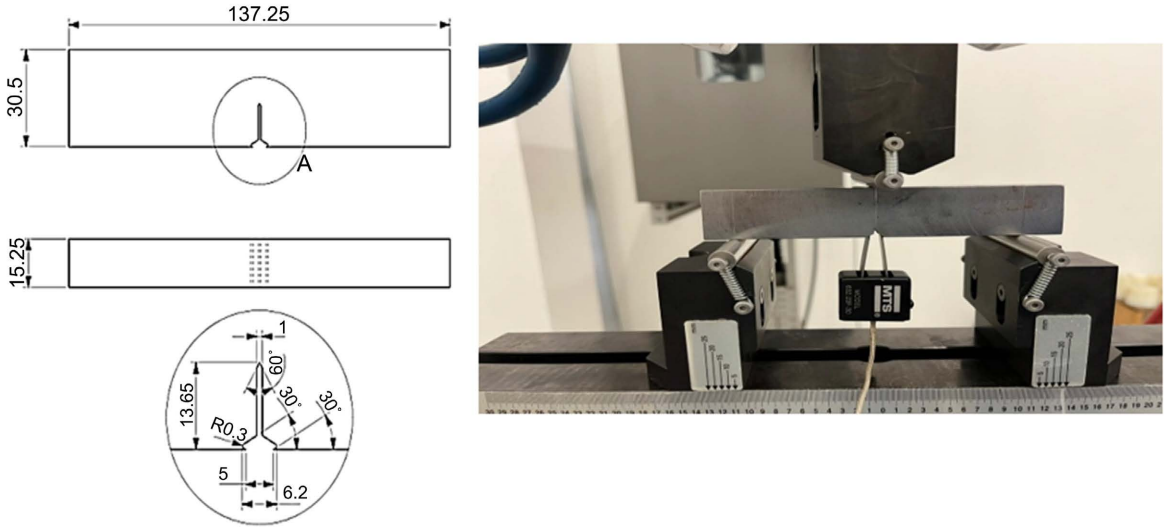

Figure 2. (a) Details of the views and dimensions of the specific samples and (b) Apparatus for carrying out the R-curve test with a sample positioned.

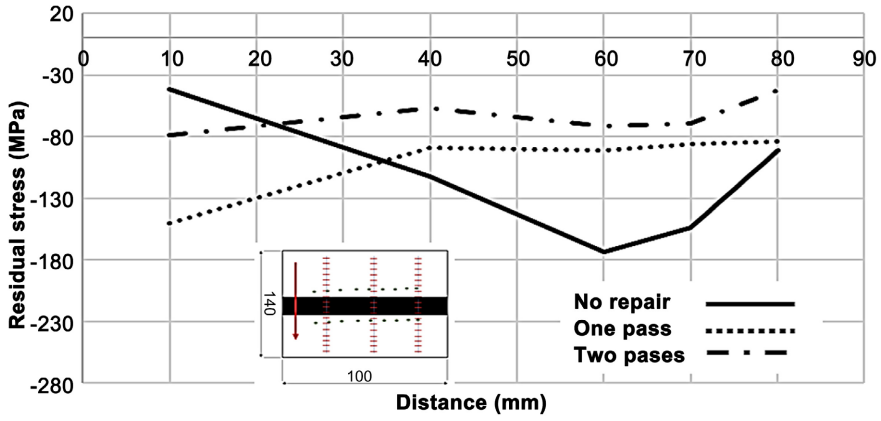

Figure 3. Results of residual stress in the transverse direction to the welding bead (along 140 mm dimension). The measurement direction is indicated in the figure.

was applied, it was noticed that the residual stress tended to become more uniform throughout the measurements, indicating that the repair provided a kind of standardization of magnitude.

A fact that draws attention is the compressive characteristic of the residual stress, something that is not expected in cases of welded regions. The same characteristic was repeated when taking longitudinal measurements in the HAZ as showed in Figure 4. With the increase in the number of repair passes, the values of the compressive residual stress have reduced.

It is observed that the residual compressive stresses are greater than the yield of the base metal (220 MPa). For this occurrence is the fact that the original sheet is cold rolled, thus presenting a characteristic of compressive residual stress on the surface, the region where the measurement was carried out.

Concerns the geometry of the K-groove adopted so that there was total welding penetration, favouring the accumulation of liquid metal in the region of the

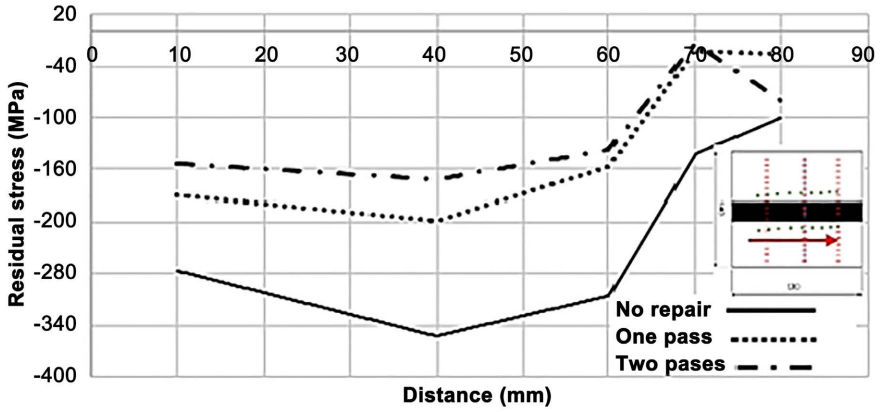

Figure 4. Results of HAZ residual stress in the direction longitudinal to the welding bead. The measurement direction is indicated in the figure.

weld pool, on the surface of the welding region. During solidification this accumulation can cause compressive residual stresses due to solidification. Therefore, the fact that the material is laminated together with the solidification characteristics caused compressive residual stress even after welding. It is also noted that as heat was added through repair, the tendency was for residual stress values to migrate towards less compressive fields.

The forming process plays an important role in the level of residual stress that is recorded in the material. As mentioned, the sheets in this study were cold rolled and because they are materials used in oil and gas piping, precisely with the intention of maintaining the compressive field to prevent the growth of defects.

Figure 5 shows the comparation of microhardness profile obtained for all conditions, with the dashed line at 3.0 mm representing Heat Affected Zone (HAZ) and the vertical dashed line the end of it. After HAZ the base material is present. The region between 0 and 3 mm represents heat affected zone (HAZ).

It can be observed that the microhardness showed little variation depending on the repair passes, but with greater uniformity the greater the number of passes. This is a positive indication since more homogeneous hardness profiles mean regions with less propensity to suffer the nucleation and propagation of cracks. It was observed that in the region of the heat-affected zone, the Vickers microhardness values changed. According to the literature [6], this may occur due to the non-uniform heating and cooling cycle due to the shielding gas flow favoring the cooling of the area where the nozzle passes through the part. With the occurrence of a repair pass, it is possible to notice that the Vickers microhardness profile tends to be more uniform (with less intense peaks) both in the HAZ and in the base metal.

This is an indication that the new thermal cycle used modified the microstructure of the material to the point of altering the residual stress values and its profile. In theory, the higher the hardness of the material, the lower its fracture toughness, so it is interpreted that the more uniform results and with smaller

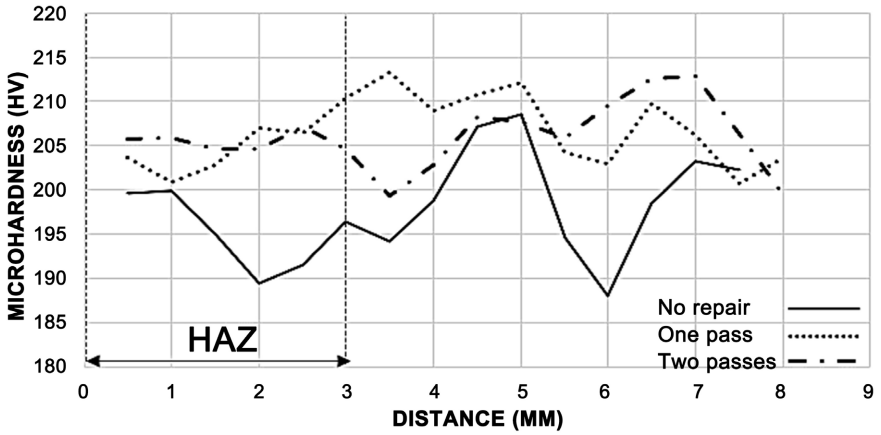

Figure 5. Microhardness results. The center of the weld bead is coordinate zero. The dotted lines indicate HAZ position.

peaks of the repaired parts bring less probability of nucleation and propagation of cracks in the regions of peak hardness.

Although at first they found value of compressive residual stress is different from the expected tensile profile, one possibility to explain these results would be the consideration that the durometer penetrates the deeper layers of the material, while the X-ray beam is absorbed on the surface of the material welded plate, reaching shallow depth and not measuring residual stress in deeper regions.

Figure 6 shows the results of the fracture test (ductile tearing) for all manufacturing conditions to determine the value of J integral in relation to the crack tip opening CMOD. For all conditions, the J curves depending on the opening at the crack mouth evolve in the same way, up to the point at which the curve drops due to the rupture of the material.

One curve to condition of one repair pass had low CMOD and low toughness. This behaviour may be associated with the presence of a discontinuity (imperfection) in the region of welded joint that helped nucleate a secondary crack and facilitated the rupture of the specimen. According to Huang [9] computational tests indicate that the presence of imperfections in the weld causes a sudden drop in the values of the J integral during the test.

Recent studies cite a drop in fatigue life of up to 98% for defects up to 3 mm and a consequent drop in crack driving force values (J integral) due to the presence of defects in the weld metal, the interface of the MB and HAZ and in the material itself [11].

The results presented in Figure 7 indicated that the welding repair did not interfere much in the R curves and the welding itself had a greater influence on the results, not showing any improvement or worsening due to the repair pass.

Figure 7 shows an example of discontinuity at the interface between the HAZ and the base metal. As the fatigue pre-crack was placed in this region, upon reaching this point, the crack or catastrophic failure occurred. It is noted that in all cases the beginning of the curves practically start together, and sudden drops in load only occur when they cross an imperfection in the weld.

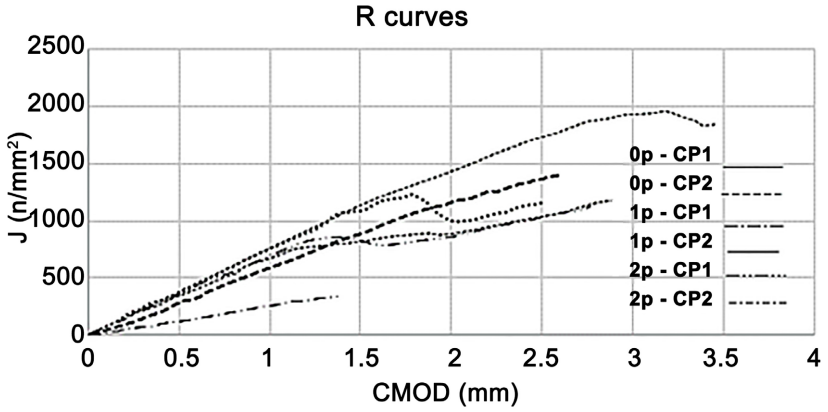

Figure 6. R-curves of welded and repaired material.

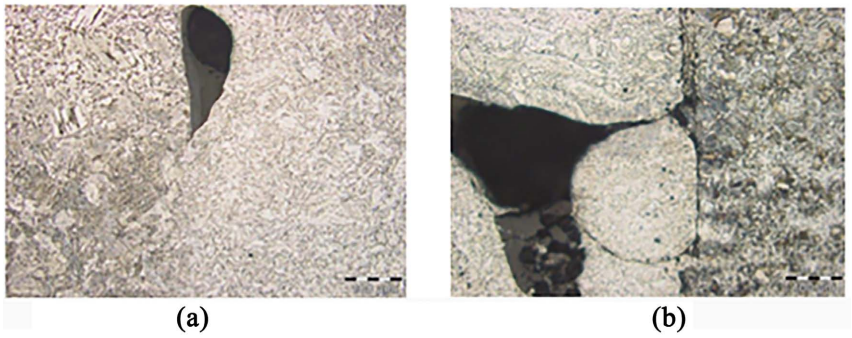

Figure 7. Imperfection at the interface of the HAZ interface. (a) and (b): lack of fusion.

To a certain extent, it can be understood that the higher the material's hardness, the greater the crack driving force and the lower the material's resistance to defects, as can be seen by the R-curves. It was noticed that the presence of discontinuities governed the crack propagation process in the R-curve test, indicating that even with the welding parameters previously studied and applied without human interference (automatic welding) eventual process defects can negatively interfere with the properties fracture of the welded joint.

Furthermore, it was noted that the slope of the load and J-integral curves are slightly different when comparing the material without repair and with one and two repair passes, differing at the stage where the rounding of the crack tip begins. At that moment it was noticed that the parts with more repair passes tended to withstand more of the load imposed in the test. The result obtained can be interpreted by the observation that: the repair does not interfere as significantly as the welding process in the resistance of the material, but it can alleviate sharp corners in the welded joint carried out in the field, which can facilitate the propagation of cracks Know—Most of the cracks are born in discontinuities on the surface of the material, so the more perfect the surface, the greater the chance of the crack not nucleating.

4. Conclusions

Welding repair of parts in the field alleviates the geometry of the bead and re-

duces reinforcement, making there less chance of cracks nucleating and propagating in the material.

The residual stress varied across the cross section of the joint, tending towards less negative values in function of the higher the repair number, showing that the repair induced stress relief in the compressive residual stress. It was observed that the welding and repair processes changed the residual stress behaviour.

Additionally, it was observed that microhardness showed stabilization in values with the greater the number of repairs passes and without repair, microhardness peaks were observed.

Finally, in relation to the values of the J integral, it was noted that the presence of discontinuities had a greater influence on the toughness values when comparing repair passes and parts without repair.

It was noticed that the geometry of the bead alone is not sufficient to determine the influence of the number of repair passes, with the greatest differences occurring between parts without repair and those with one repair pass.

Acknowledgements

CAPES, IPEN and Prof. Dr Diego Burgos (POLI-USP Naval and Oceanic) and Prof. Dr Rene Oliveira (IPEN-USP).

Conflicts of Interest

The authors declare no conflicts of interest regarding the publication of this paper.

References

[1] Anderson, T.L. (2017) Fracture Mechanics: Fundamentals and Applications. 3rd Edition. Boca Raton, Florida.

[2] (2018) ASTM E1820: Standard Test Methods for Fracture Testing of Metallic Materials. https://www.astm.org/e1820-20.html

[3] Vajari, K.K. and Saffar, S. (2022) Investigation of Gas Tungsten Arc Welding Parameters on Residual Stress of Heat Affected Zone in Inconel X750 Super Alloy Welding Using Finite Element Method. *ICPEM* 2022: *International Conference on Product Engineering and Manufacturing*, Toronto, 20-21 September 2022.

[4] Nyembwe, K.J., Ashiegbu, D.C. and Potgieter, H.J. (2022) Gas Phase Extraction: An Environmentally Sustainable and Effective Method for the Extraction and Recovery of Metal from Ores. *ICMEH* 2023: *International Conference on Metallurgical Engineering and Hydrometallurgy*, Paris, 17-18 May 2023. https://waset.org/metallurgical-engineering-and-hydrometallurgy-conference-in-may-2023-in-paris?utm_source=conferenceindex&utm_medium=referral&utm_campaign=listing

[5] Lathitnen, T. and Vilaça, P. (2019) Fatigue Behavior of MAG Welds of Thermomechanically Processed 700MC Ultra High Strength Steel. *International Journal of Fatigue*, **126**, 62-71. https://doi.org/10.1016/j.ijfatigue.2019.04.034

[6] Nunes, T.S., Alves, J.M. and Brandão, L.P.M. (2022) Distribuição de tensão residual em chapas laminadas a frio. 57° *Seminário de Laminação e Conformação de Metais*,

57, 511-522. https://doi.org/10.5151/2594-5297-34974

[7] Dantas, S.S. (2013) Influência da profundidade de trinca e restrição à plasticidade da avaliação experimental de tenacidade à fratura (J E CTOD) de aço ASTM A516 grau 70. Master's Thesis, Centro Universitário da FEI, São Bernardo do Campo.

[8] Yang, X., Chen, H., Zhu, Z., *et al.* (2019) Effect of Shielding Gas Flow on Welding Process of Laser-Arc Hybrid Welding and MIG Welding. *Journal of Manufacturing Processes*, **38**, 530-542. https://doi.org/10.1016/j.jmapro.2019.01.045

[9] Huang, T., Mario, M., Minnaar, K., Gioielli, P., Kibey, S. and Fairchild, D. (2011) Development of the SENT Test for Strain-Based Design of Welded Pipelines. 2010 8*th International Pipeline Conference*, Calgary, 27 September-1 October 2010, 303-312. https://doi.org/10.1115/IPC2010-31590

[10] Tomkow, J., Rogalski, G., Fydrych, D., *et al.* (2018) Improvement of S355G10+N Steel Weldability in Water Environment by Temper Bead Welding. *Journal of Materials Processing Technology*, **262**, 372-381. https://doi.org/10.1016/j.jmatprotec.2018.06.034

[11] Xu, X., Xie, L., Zhou, S., An, J., Huang, Y., Liu, Y. and Jin, L. (2023) Effect of Welding Defects on Fatigue Properties of SWA490BW Steel Cruciform Welded Joints. *Materials*, **16**, 4751. https://doi.org/10.3390/ma16134751